The Plant Cell, Vol. 26: 4328–4344, November 2014, www.plantcell.org

A DEK Domain-Containing Protein Modulates Chromatin Structure and Function in *Arabidopsis*[W][OPEN]

Sascha Waidmann,[a] Branislav Kusenda,[a] Juliane Mayerhofer,[a] Karl Mechtler,[b] and Claudia Jonak[a,1]

[a] Gregor Mendel Institute of Molecular Plant Biology, Austrian Academy of Sciences, Vienna Biocenter, 1030 Vienna, Austria
[b] Research Institute of Molecular Pathology, Vienna Biocenter, 1030 Vienna, Austria

Chromatin is a major determinant in the regulation of virtually all DNA-dependent processes. Chromatin architectural proteins interact with nucleosomes to modulate chromatin accessibility and higher-order chromatin structure. The evolutionarily conserved DEK domain-containing protein is implicated in important chromatin-related processes in animals, but little is known about its DNA targets and protein interaction partners. In plants, the role of DEK has remained elusive. In this work, we identified DEK3 as a chromatin-associated protein in *Arabidopsis thaliana*. DEK3 specifically binds histones H3 and H4. Purification of other proteins associated with nuclear DEK3 also established DNA topoisomerase 1α and proteins of the cohesion complex as in vivo interaction partners. Genome-wide mapping of DEK3 binding sites by chromatin immunoprecipitation followed by deep sequencing revealed enrichment of DEK3 at protein-coding genes throughout the genome. Using DEK3 knockout and overexpressor lines, we show that DEK3 affects nucleosome occupancy and chromatin accessibility and modulates the expression of DEK3 target genes. Furthermore, functional levels of DEK3 are crucial for stress tolerance. Overall, data indicate that DEK3 contributes to modulation of *Arabidopsis* chromatin structure and function.

INTRODUCTION

In the nucleus of eukaryotes, DNA is tightly packed into chromatin. The chromatin structure has profound implications on gene expression, DNA replication, and repair, and it plays an important role in diverse processes, including development and responses to environmental changes (Ho and Crabtree, 2010; Li and Reinberg, 2011; van Zanten et al., 2012; Gentry and Hennig, 2014; Han and Wagner, 2014). Genomic DNA is wrapped around histone octamers to form nucleosomes, the primary level of chromatin organization. Histone octamers consist of two molecules each of histones H2A, H2B, H3, and H4. The linker histone H1 organizes the nucleosome arrays into more condensed fibers. A multitude of diverse proteins such as histone chaperones, histone-modifying enzymes, ATP-dependent chromatin remodeling complexes, and nonhistone architectural proteins alter local chromatin properties and/or affect higher order chromatin structure (Ho and Crabtree, 2010; Luger et al., 2012; Gentry and Hennig, 2014).

The evolutionarily conserved DEK protein has been implicated in the regulation of multiple chromatin-related processes (Waldmann et al., 2004; Riveiro-Falkenbach and Soengas, 2010; Broxmeyer et al., 2013; Privette Vinnedge et al., 2013). DEK was first described in humans as affected by a chromosomal translocation in a subset of patients with myeloid leukemia and was named after the initials of the patient (von Lindern et al., 1990; Soekarman et al., 1992). DEK is a bona fide oncoprotein (Wise-Draper et al., 2009) and is associated with a number of different types of tumors (Riveiro-Falkenbach and Soengas, 2010). DEK is also associated with stem and progenitor cell qualities (Broxmeyer et al., 2012). DEK has no known enzymatic activity, but biochemical studies revealed DNA, chromatin, and histone binding as well as DNA-folding activities for DEK, classifying DEK as an architectural chromatin protein (Alexiadis et al., 2000; Waldmann et al., 2002, 2003; Kappes et al., 2004a, 2004b, 2008, 2011; Tabbert et al., 2006; Gamble and Fisher, 2007; Sawatsubashi et al., 2010).

In vitro DEK-DNA binding studies showed a preferential binding of recombinant DEK to supercoiled and cruciform DNA (Waldmann et al., 2003). Other analyses indicated sequence-specific binding of human DEK (Hs-DEK) to DNA (Fu et al., 1997; Faulkner et al., 2001; Adams et al., 2003), and *Drosophila melanogaster* DEK (Dm-DEK) was found associated with the nuclear ecdysone receptor locus (Sawatsubashi et al., 2010). However, the global distribution of DEK on chromatin has remained unclear.

Recently, DEK was shown to have histone chaperone activity in vitro (Sawatsubashi et al., 2010; Kappes et al., 2011) and to be important for heterochromatin integrity (Kappes et al., 2011). Furthermore, DEK was implicated in DNA replication (Alexiadis et al., 2000), DNA double-strand break repair (Kappes et al., 2008; Kavanaugh et al., 2011), mRNA splicing (Le Hir et al., 2000, 2001; McGarvey et al., 2000; Soares et al., 2006), and transcriptional regulation (Campillos et al., 2003; Sammons et al., 2006; Gamble and Fisher, 2007; Sawatsubashi et al., 2010; Kappes et al., 2011).

While DEK has been associated with various functions in animals, the biological role of DEK in plants remained elusive, although the gene underwent multiplication and diversification. In *Arabidopsis thaliana*, four genes code for DEK proteins: *DEK1*, *DEK2*, *DEK3*, and *DEK4* (Pendle et al., 2005). Based on publically available microarray data indicating strong and abundant expression of DEK3, we selected DEK3 for characterization. In this study, we provide evidence that DEK3 is a plant chromatin protein

[1] Address correspondence to claudia.jonak@gmi.oeaw.ac.at.
The author responsible for distribution of materials integral to the findings presented in this article in accordance with the policy described in the Instructions for Authors (www.plantcell.org) is: Claudia Jonak (claudia.jonak@gmi.oeaw.ac.at).
[W] Online version contains Web-only data.
[OPEN] Articles can be viewed online without a subscription.
www.plantcell.org/cgi/doi/10.1105/tpc.114.129254

involved in regulating nucleosome occupancy and gene expression. We present two complementary global analyses to provide a more systematic view on the functions of DEK. Moreover, we identified DEK3 as a regulator of stress tolerance in *Arabidopsis thaliana*.

RESULTS

Domain Structure of the At-DEK3 Protein

Human DEK protein harbors two DNA binding domains: the SAP (Scaffold attachment factor A/B-Acinus-Pias) box, a DNA binding motif present in a number of chromatin-associated proteins, and the C-terminal DEK domain (Waldmann et al., 2004). Both domains are conserved in At-DEK3. To identify the SAP box in At-DEK3, the protein was aligned together with human DEK and two published SAP box consensus sequences (Aravind and Koonin, 2000; Kipp et al., 2000). Like human DEK, At-DEK3 contains a centrally located SAP box consisting of a bipartite region of conserved hydrophobic, aliphatic, and acidic residues (Figure 1A). To identify the DEK domain in At-DEK3, we first aligned all 606 entries of proteins annotated with a putative DEK domain in the Pfam protein database (Punta et al., 2012) and identified a putative consensus sequence for the DEK domain (Figure 1A). Similar to Hs-DEK, the DEK domain is located at the C terminus of At-DEK3.

Nuclear Localization of At-DEK3

DEK is ubiquitously and highly expressed in rapidly proliferating animal cells (Waldmann et al., 2004; Privette Vinnedge et al., 2013). In line with a role of At-DEK3 in dividing cells, *DEK3* was highly expressed in young *Arabidopsis* seedlings (Supplemental Figure 1A).

To study the subcellular localization of DEK3, localization of a DEK3-CFP (cyan fluorescent protein) fusion protein was first investigated in transiently transformed tobacco (*Nicotiana tabacum*) leaves. CFP fluorescence was exclusively detected in the nucleus (Supplemental Figure 1B). Consistent with the transient expression data, nuclear fluorescence was also observed in *Arabidopsis* plants stably transformed with a DEK3-CFP fusion and observed fluorescence in nuclei (Figure 1B). To confirm this subcellular localization, we performed protein gel blot analysis with total protein, cytosolic, and nuclear extracts. Consistent with the microscopic analyses, DEK3 protein was detected in total and nuclear, but not in cytosolic protein extracts (Figure 1C).

DEK3 Interaction with Histones H3 and H4

Hs-DEK and Dm-DEK proteins interact with histones (Alexiadis et al., 2000; Sawatsubashi et al., 2010; Kappes et al., 2011). To analyze whether At-DEK3 shares this feature, we performed far-Western blot analyses. Membranes with electrophoretically separated core histones were incubated with purified, recombinant glutathione *S*-transferase (GST)-DEK3 protein and subsequently with GST antibodies. At-DEK3 interacted specifically with histones H3 and H4 (Figure 2A); no signal was observed for histones H2A and H2B.

To investigate whether DEK3 interacts with core histones in planta, we performed coimmunoprecipitation experiments. DEK3 was immunoprecipitated with green fluorescent protein (GFP) antibodies from nuclear extracts of seedlings expressing DEK3-CFP. Subsequently, protein gel blot analysis was performed using antibodies against the histones H2A, H2B, H3, and H4. In line with the in vitro binding assays, DEK3 coimmunoprecipitated in vivo only with histones H3 and H4 (Figure 2B).

DEK3 Association with Topoisomerase 1α and Cohesin Components in Vivo

To investigate the role of DEK3 in the nucleus, we identified proteins associated with DEK3 using immunoaffinity purification followed by mass spectrometry. Nuclear extracts from 2-week-old soil-grown plants expressing DEK3-CFP were used to purify DEK3-associated proteins with GFP antibodies. Wild-type plants were used as control. The analysis was repeated three times with independently grown plant material. Proteins that were identified in at least two coprecipitation analyses from DEK3-CFP nuclear extracts but not in any of the wild-type samples were considered to be DEK3 copurifying factors.

We identified 17 proteins that consistently coimmunoprecipitated with DEK3 (Table 1). Many of the DEK3-associated proteins are involved in DNA-dependent processes. DNA topoisomerase 1α (Top1α; Kieber et al., 1992) copurified in all three experiments with DEK3. Top1α is a type I DNA topoisomerase involved in DNA replication, recombination, repair, and transcription (Wang, 2002; Leppard and Champoux, 2005), and *Arabidopsis* Top1α is involved in development (Takahashi et al., 2002; Graf et al., 2010). Among the other proteins copurifying with DEK3 were the cohesion protein SCC3 involved in mitotic and meiotic cell division (Chelysheva et al., 2005; Schubert et al., 2009) and a putative homolog of the cohesion-associated protein PDS5. Nitrilase1, a multifunctional protein implicated in cytokinesis and in maintaining genome stability (Doskočilová et al., 2013), was also identified in all experiments. Further, histone deacetylase 3 (HDA3/HDT1) copurified with DEK3, confirming a similar interaction observed in human cells (Hollenbach et al., 2002). DEK3-associated proteins also comprised two yet uncharacterized proteins with a PWWP domain, a structural module characteristic of chromatin regulators, two DNA binding storekeeper protein-related transcriptional regulators of unknown biological function and Short Life 1, a putative transcription factor with a PHD finger, and a BAH motif involved in developmental regulation (Müssig et al., 2000). We also identified DEK4, indicating that DEK3 might form heterodimers with DEK4. Furthermore, DEK3 pulled down an F-box protein, which is interesting because in mice, DEK protein levels can be regulated by the F-box protein FBXW7 (Babaei-Jadidi et al., 2011). Two other copurified proteins involved in plant stress tolerance are discussed below.

To validate the quality of the DEK3 coimmunopurification analyses, we selected At-SSC3 for which specific antibodies are available (Chelysheva et al., 2005) and performed inverse coimmunoprecipitation experiments. After immunoprecipitating nuclear protein extracts of wild-type and DEK3-CFP-expressing plants with the SCC3 antibodies and protein gel blot analysis with GFP antibodies (Figure 3A), we could demonstrate that

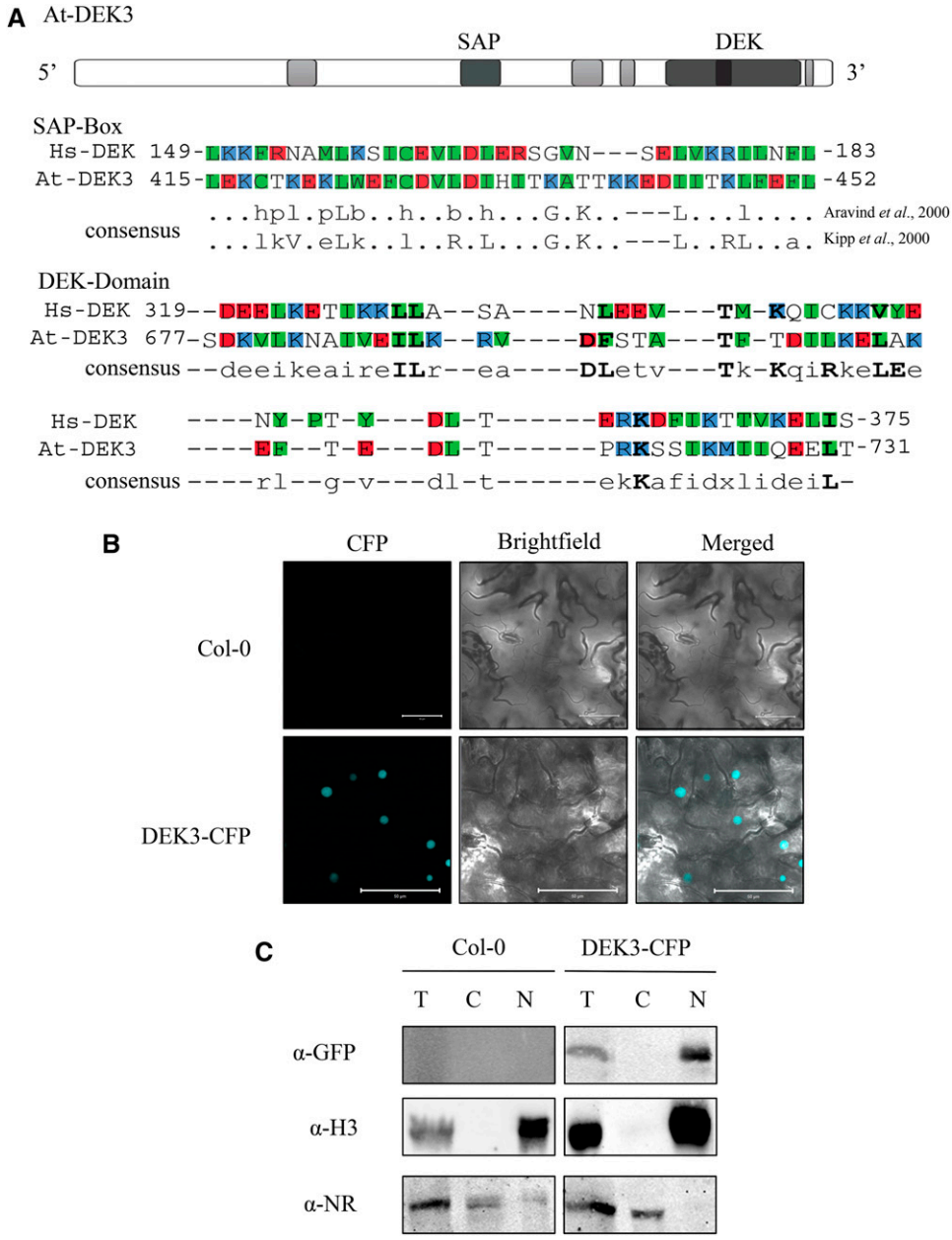

Figure 1. Domain Structure and Nuclear Localization of At-DEK3.

(A) Top panel: Schematic diagram of At-DEK3 indicating the SAP and DEK domain. Middle panel: Alignment of SAP domains of human DEK (Hs-DEK) and *Arabidopsis* DEK3 (At-DEK3) with two consensus sequences (Aravind and Koonin, 2000; Kipp et al., 2000). Lower panel: Alignment of DEK domains of human DEK (Hs-DEK) and *Arabidopsis* DEK3 (At-DEK3) with a consensus sequence identified by aligning all proteins with a putative DEK domain annotated in the Pfam database (Punta et al., 2012). Alignments were generated with the CLC Main Workbench 6 using a progressive alignment algorithm (Edgar and Batzoglou, 2006). Bold letters in the consensus sequence are conserved in more than 60% of all entries in the database. The code indicates hydrophobic (H) or aliphatic amino acids (L) colored in green, acidic residues (Glu [E] and Asp [D]) colored in red, and basic residues (Arg [R], His [H], and Lys [L]) colored in blue.
(B) Subcellular localization of DEK3 protein in *Arabidopsis* seedlings stably transformed with DEK3-CFP (lower panel). Fourteen-day-old seedlings of line 9-1 were analyzed by confocal microscopy. The distribution of the CFP signal is representative of several independent plant lines. Nontransformed wild-type Col-0 plants were used as control (upper panel). Bars = 50 μm.
(C) Protein gel blot analysis of *A. thaliana* total (T), cytosolic (C), and nuclear (N) protein extracts from 14-d-old wild-type Col-0 and DEK3-CFP-expressing seedlings (line 9-1). DEK3-CFP protein was detected with GFP antibodies. Antibodies against histone H3 (α-H3) and nitrate reductase (α-NR) were used as nuclear and cytosolic markers, respectively.

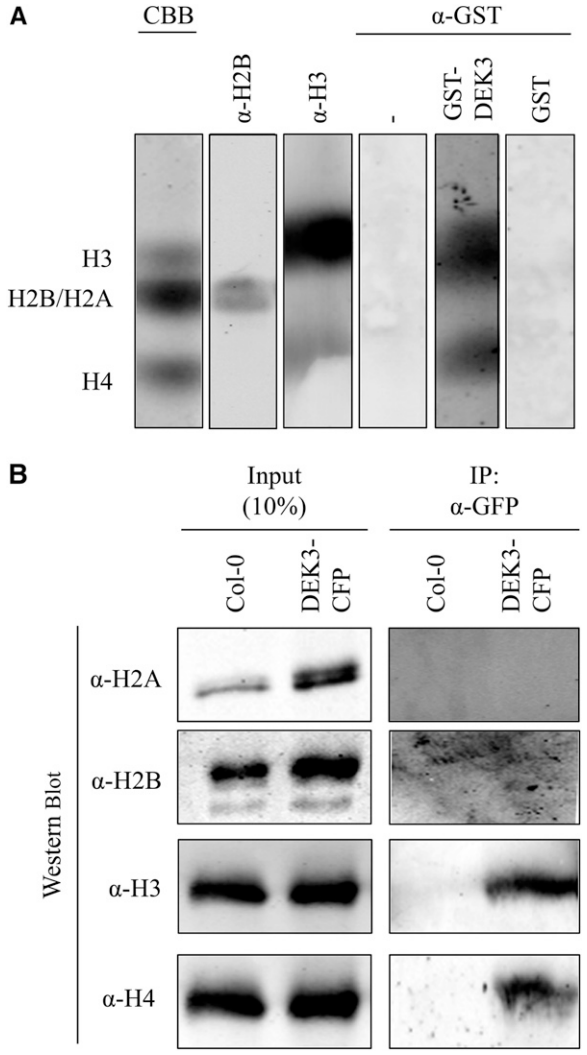

Figure 2. Interaction of DEK3 with Histone H3 and H4 in Vitro and in Vivo.

(A) Purified recombinant GST-DEK3 directly binds to histone H3 and H4 in far-Western blot analysis. Histones were separated by SDS-PAGE. One lane of the blotted membrane was stained with Coomassie blue (CBB). Other lanes were incubated with either 100 ng/cm^2 GST-DEK3 or GST alone prior to protein gel blot with GST antibodies. As controls, membranes were incubated with H2B or H3 antibodies.

(B) DEK3-CFP coimmunoprecipitates with histones H3 and H4 in vivo. Nuclear extracts of 14-d-old wild-type Col-0 and DEK3-CFP-expressing seedlings (line 9-1) were used in immunoprecipitations (IP) with GFP antibodies. Immunoprecipitated proteins were subjected to protein gel blot analyses using antibodies against histones H2A, H2B, H3, and H4. Ten percent of the inputs were used as positive controls (left panel).

DEK3-CFP copurified with SCC3, confirming that both proteins are associated in vivo.

Intriguingly, Top1α was found to be associated with DEK3. TopI enzymes are essential for relaxing DNA supercoiling generated by transcription, replication, and chromatin remodeling (Wang, 2002; Leppard and Champoux, 2005). Hs-DEK protein has DNA supercoiling activity in vitro in the presence of TopI (Alexiadis et al., 2000; Waldmann et al., 2002). This prompted us to investigate whether At-DEK3 possesses supercoiling activity. Indeed, purified recombinant DEK3 enhanced the production of supercoiled DNA in the presence of TopI (Figure 3B). Thus, the in vivo association of DEK3 with Top1α, together with the ability of DEK3 to change DNA structure in vitro, suggest that DEK3 might have the potential to modulate DNA topology in planta.

Genome-Wide Mapping of DEK3 Binding Sites

The ability of DEK3 to bind histones and to change the superhelical structure of DNA in vitro and the copurification of DEK3 with proteins involved in chromatin-related processes from plants prompted us to investigate the global distribution of DEK3 along the genome. We performed chromatin immunoprecipitations using GFP antibodies followed by deep sequencing (ChIP-Seq) with three independent transgenic DEK3-CFP plant lines. Reads were mapped uniquely to the *Arabidopsis* genome (Supplemental Table 1). To identify DEK3 DNA binding sites, we determined peaks shared by the three independent DEK3-CFP plant lines. Though there was variability between the three independent transgenic lines, we identified 577 DEK3-associated sequences corresponding to 161 genes distributed all over the five chromosomes (Supplemental Figure 2 and Supplemental Data Set 1). Interestingly, for all genes, DEK3 was enriched at least at three different sites within the gene. Gene Ontology term classification of genes enriched for DEK3 binding indicated that DEK3 target genes are involved in diverse biological processes.

The majority of DEK3 binding sites located at protein-coding genes (79%). Thirty-four percent of the DEK3 binding sites were found in exons and 19% in introns (Figure 4A), which is similar to the fractions of genomic regions in the *Arabidopsis* genome (31% exons and 18% introns; Lawson and Zhang, 2006). However, the number of DEK3 peaks was increased in 5′ untranslated regions (UTRs) (12%) and 3′ UTRs (14%) and decreased in intergenic regions (21%) compared with the genome-wide fractions of 4, 2, and 45%, respectively. We next investigated the enrichment profile of DEK3 over protein-coding gene regions and their flanking 5′ and 3′ sequences (Figure 4B). DEK3 was enriched over gene bodies and the binding signal further increased in a 2-kb region upstream of the translational start site (ATG) and in a 1-kb region downstream of the translational termination site (stop codon).

To validate the ChIP-Seq analysis, we performed ChIP-quantitative PCR (ChIP-qPCR) analyses from three independent immunoprecipitations of three independent DEK3-CFP lines. We selected *DEK3* itself, *Top1α*, and *PDS5* as genes encoding DEK3-interacting proteins and three additional gene loci binding DEK3 at the DNA level (*MBD9*, Methyl-CpG binding domain 9; *HKL1*, Hexokinase-like 1; *EFS*, Early Flowering in Short Days). All but one of 29 tested regions were confirmed to be enriched for DEK3 in at least two of the three lines (Figure 5; Supplemental Figure 3), whereas no enrichment was detected in wild-type control plants for DEK3-CFP (Supplemental Figure 4), verifying a low false positive rate for the ChIP-Seq procedure.

Table 1. Proteins Identified to Interact with DEK3

Identified Protein	Accession No.	Molecular Mass (kD)	No. of Unique Identified Peptides IP1-IP2-IP3	Protein Identification Probability (%) IP1-IP2-IP3
DNA TOP1α	At5g55300	103	5-5-4	100-100-100
DNA binding storekeeper protein-related transcriptional regulator (Store1)	At1g61730	41	4-3-7	100-100-100
Salt tolerance-related protein	At1g13930	16	3-3-6	100-100-100
Sister-chromatid cohesion protein 3 (SCC3)	At2g47980	126	2-3-3	100-100-100
Nitrilase1 (NIT1)	At3g44310	38	2-3-3	100-100-100
Rotamase CYP3 (ROC3)	At2g16600	18	2-4-2	100-100-100
Sister-chromatid cohesion protein PDS5	At5g47690	181	24-0-26	100-100-100
DNA binding storekeeper protein-related transcriptional regulator (Store4)	At4g25210	40	7-0-7	100-100-100
PWWP domain protein	At5g40340	114	0-5-3	100-100-100
DEK4	At5g55660	87	5-0-5	100-100-100
Heat shock protein 70 (HSP70)	At3g09440	71	3-4-0	100-100-100
F-box family protein	At1g20940	75	0-3-3	100-100-100
HDA3	At3g44750	26	2-0-2	100-100-100
Short Life 1 (SHL1)	At4g39100	26	2-2-0	100-100-100
Cold-responsive protein 6.6 (COR6.6)/KIN2	At5g15970	7	2-3-0	100-100-100
PWWP domain protein	At3g09670	79	0-2-2	100-100-100
Ribosomal protein large subunit 16A (RPL16A)	At2g42740	21	2-2-0	100-100-100

DEK3 was immunoprecipitated with GFP antibodies from DEK3-CFP-expressing plants, and DEK3-associated proteins were subsequently identified by mass spectrometry. Three independent biological replicates (IP1-3) were performed. Proteins identified in DEK3-CFP but not in Col-0 wild-type seedlings are shown.

Expression of DEK3 Target Genes in DEK3 Mutants

We hypothesized that the enrichment of DEK3 at protein-coding genes might influence the expression of these genes. To test this, we analyzed the transcript levels of selected DEK3 targets in wild-type Columbia-0 (Col-0), *dek3* knockout mutants (Supplemental Figures 1C and 1D), and in plants overexpressing DEK3-CFP (Supplemental Figures 1D and 1E) by reverse transcription-quantitative PCR (RT-qPCR) analysis (Figure 6). In *dek3* mutants, expression levels of *Top1α*, *EFS*, *MBD9*, *NUP160* (Nucleoporin 160), *DEK1* (Defective kernel 1), auxin transport protein *BIG* (also known as *ASA1*; Attenuated shade avoidance 1), *HB-1* (Homeobox 1), and *CMT3* (Chromomethylase 3) were elevated to different extents, whereas in DEK3 overexpressors, transcript levels were reduced compared with wild-type plants. We observed that transcript levels of *HKL1* and *PDS5* were reduced in *dek3* and in DEK3-overexpressing plants, suggesting that DEK3 might regulate gene expression indirectly or in a locus-specific manner.

Influence of DEK3 Levels on Nucleosome Occupancy and DNA Accessibility

The observations that DEK3 binds to chromatin and that levels of DEK3 influence gene expression in *Arabidopsis* plants raised the question whether DEK3 might be involved in regulating DNA accessibility. Therefore, we first investigated histone H3 occupancy at the *Top1α* and the *MBD9* loci by chromatin immunoprecipitation (ChIP) analysis using histone H3 antibodies. In plants with elevated DEK3 levels, histone H3 occupancy was strongly increased throughout the *Top1α* gene region, whereas H3 occupancy was similar or lower in plants deficient in DEK3 (Figure 7A). Similarly, histone H3 occupancy was enhanced throughout the *MBD9* locus in DEK3 overexpressing but reduced in *dek3* plants (Supplemental Figure 5A), suggesting that nucleosome density can be modified by DEK3 levels.

We also assessed nucleosome density by a nuclease sensitivity-based assay. We digested nuclei from wild-type Col-0 and plants deficient for or overexpressing DEK3 with MNase I (which preferentially digests naked DNA), isolated mononucleosomal DNA, and analyzed the *Top1α* and the *MBD9* gene regions by quantitative PCR (qPCR). In line with the histone H3 ChIP data, markedly more PCR product was detected at each of the tested sites of the *Top1α* and the *MBD9* loci in DEK3 overexpressor lines, and lower levels were amplified in *dek3* compared with the wild type (Figure 7B; Supplemental Figure 5B), suggesting that DEK3 promotes nucleosome density.

To further confirm the influence of DEK3 on DNA accessibility, we performed CHART-PCR (chromatin accessibility by real-time PCR) and digested nuclei from Col-0, *dek3*, and DEK3 overexpressor plants with MNase I followed by qPCR analysis of different regions of the *Top1α* and the *MBD9* locus. Consistent with the previous analyses, we observed a strongly increased MNase accessibility in DEK3-deficient plants, whereas MNase accessibility was reduced in DEK3 overexpressor plants (Figure 7C; Supplemental Figure 5C). At control regions, histone H3 occupancy, nucleosome density, and DNA accessibility were generally similar in wild-type, DEK3 overexpressor, and knockout mutants (Supplemental Figure 6). Taken together, these results clearly indicate that DEK3 can modulate nucleosome occupancy and has the potential to alter chromatin accessibility.

Role of DEK3 and Top1α in Salt Stress Tolerance

Among the proteins associated with DEK3, we identified a salt tolerance-related protein (Du et al., 2008) and the stress-induced

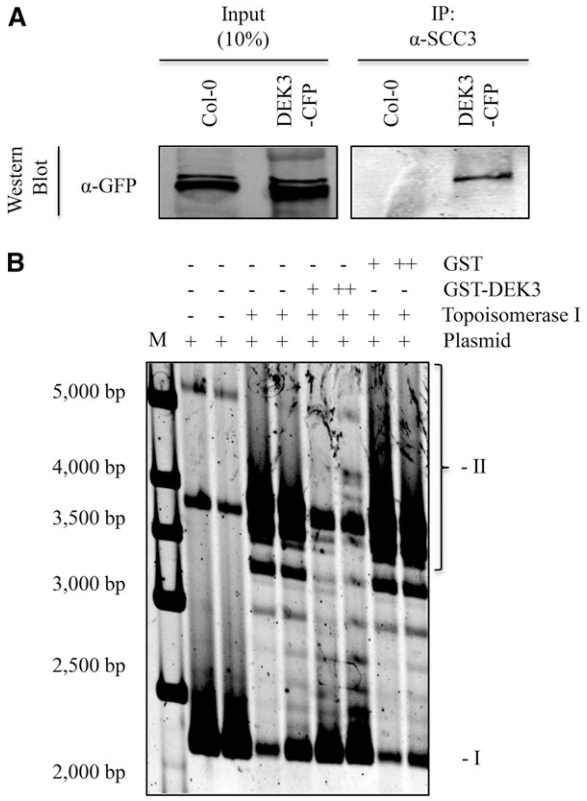

Figure 3. DEK3 Interaction with SSC3 and Change of DNA Topology.

(A) SCC3 copurifies with DEK3. SCC3 was immunoprecipitated from 14-d-old DEK3-CFP-overexpressing (line 9-1) and wild-type Col-0 seedlings. Immunoprecipitated proteins were subjected to protein gel blot analyses using GFP antibodies. Ten percent of the inputs were used as positive controls (left panel).

(B) DEK3 can change the superhelical density of DNA. Plasmid DNA was incubated with increasing amounts of GST-DEK3 in the presence of topoisomerase I. Purified DNA was analyzed by agarose gel electrophoresis and SYBR Green I staining. The positions of DNA form I (supercoiled) and II (relaxed, closed circular, and nicked DNA) are indicated. A DNA size marker is shown on the left (M).

COLD-RESPONSIVE PROTEIN 6.6 (COR6.6)/KIN2 (Kurkela and Borg-Franck, 1992; Kreps et al., 2002). This prompted us to investigate whether DEK3 might be involved in the *Arabidopsis* stress response. First, we analyzed the expression of DEK3 in plants exposed to high salinity, a major stress for plants. RT-qPCR analysis showed that *DEK3* expression was strongly and rapidly downregulated by salt stress in shoots and roots (Figure 8A).

We next analyzed whether DEK3 is important for tolerance to salt stress. Under high salinity conditions, plants deficient in DEK3 germinated significantly better compared with wild-type plants. In contrast, germination efficiency under the same conditions was significantly reduced in plants overexpressing DEK3 (Figure 8B). Overexpression of DEK3-CFP in *dek3* mutant background reverted the *dek3* stress tolerance phenotype (Figure 8B). Furthermore, *dek3* seedlings transferred from normal to high salinity conditions were hypersensitive to salt stress (Figure 8E), indicating that DEK3 levels are critical for salt stress tolerance.

Given that Top1α copurified with DEK3, and DEK3 levels regulate the expression of *Top1α*, we asked whether Top1α plays a role in salt stress tolerance. Indeed, *Top1α* transcript levels were strongly reduced in roots and leaves after short-term salt stress (Figure 8C). Also, *top1α* mutants (Supplemental Figures 7A and 7B) were significantly more resistant to high salinity conditions (Figure 8D) compared with the wild type. These results indicate that DEK3 and Top1α are negative regulators of salt stress tolerance and play a role in the same biological process. Additionally, *dek3 top1α* double knockout plants showed a similar sensitivity to salt as single *top1α* mutants (Figure 8E), suggesting that DEK3 and Top1α are part of the same pathway.

DISCUSSION

Chromatin-associated proteins determine chromatin structure and function and thereby regulate a multitude of cellular processes.

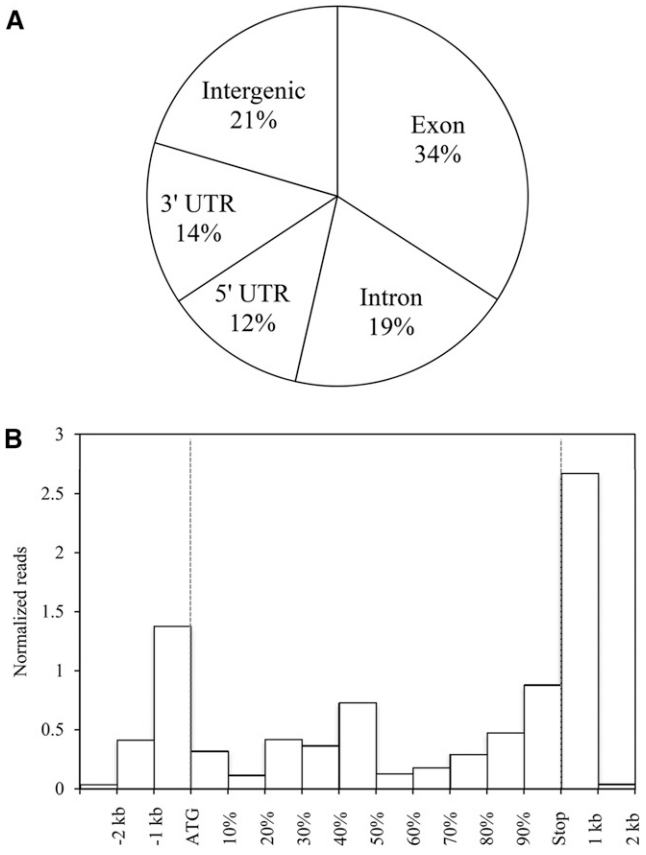

Figure 4. Genome-Wide Identification of DEK3 Binding Sites.

(A) Percentage of DEK3 binding sites in exons, introns, 1 kb upstream of ATG, 1 kb downstream of the stop codon, and in intergenic regions of all 577 sites enriched for DEK3.

(B) Distribution of DEK3 binding sites relative to the gene structure. For each gene, reads were summed according to their positions in 1-kb windows from 3 kb upstream of the start codon to the start codon and from the stop codon 2 kb downstream of the stop codon. Within the gene bodies, reads were summed according to their positions in windows equal to 10% of the gene length. All reads were normalized by the total number of reads and peaks. ATG, start codon. Stop, translation termination site.

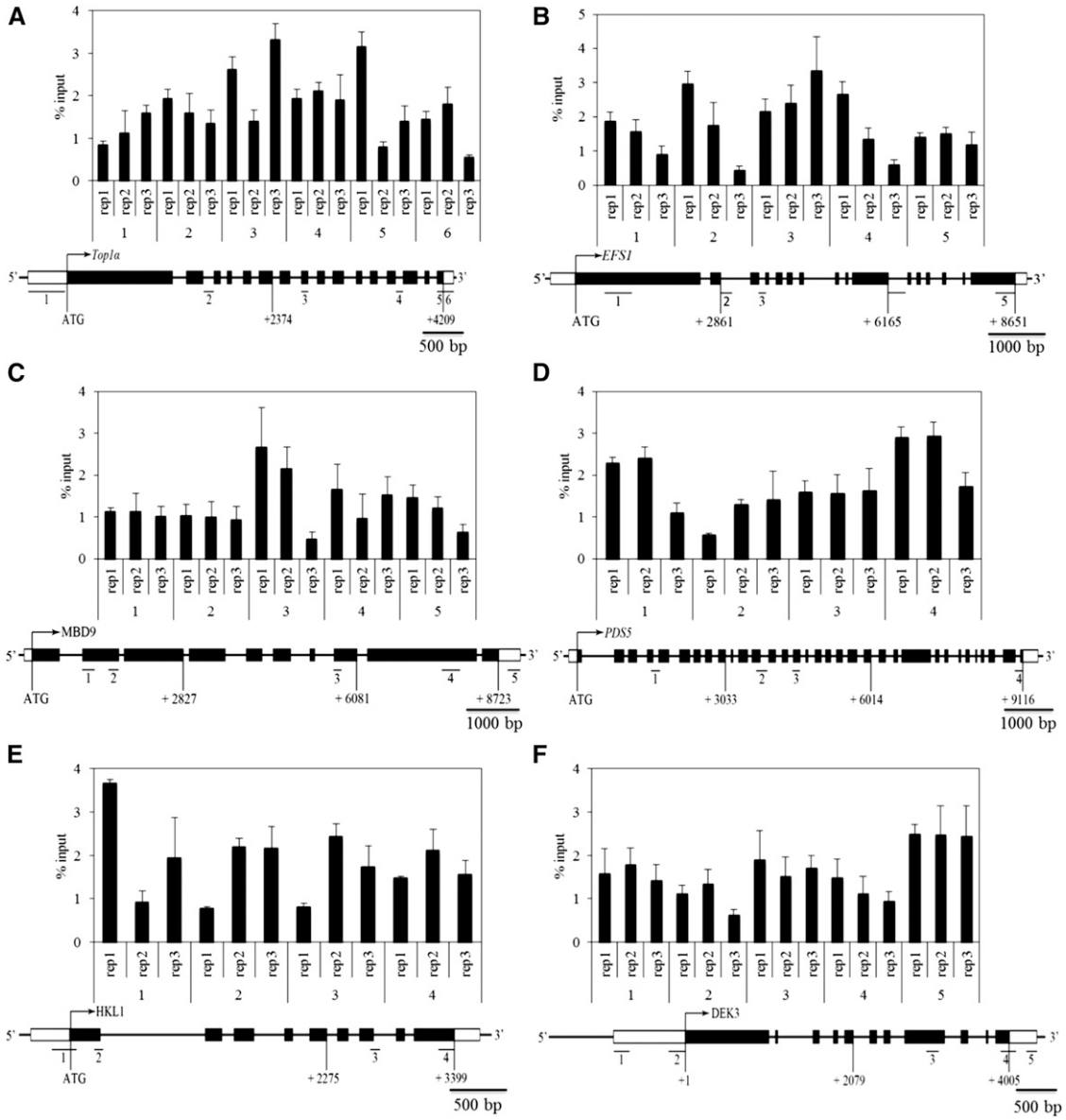

Figure 5. ChIP-qPCR Verification of Specific DEK3 Binding Sites.

Schematic diagrams below the bar graphs illustrate the genomic regions analyzed, with CDS (black boxes) and UTRs (white boxes). Short bars with numbers indicate specific sites analyzed for DEK3 binding. The bar graphs illustrate the relative enrichment of DNA association with DEK3 over the input control. Data of three biological replicates generated with the DEK3-CFP line 9-1 are shown. Data are means ± relative SD of three technical measurements. A scale bar for each gene is shown. **(A)** *Top1*α locus, **(B)** *EFS1* locus, **(C)** *MBD9* locus, **(D)** *PDS5* locus, **(E)** *HKL1* locus, and **(F)** *DEK3* locus.

DEK is implicated in important chromatin-related processes in animals, but little is known about its DNA targets and its protein interaction partners. In plants, the function of DEK has remained unclear. In this work, we identified DEK3 as a chromatin-associated protein in *Arabidopsis*. A combination of global approaches with detailed biochemical, molecular, and genetic analyses indicate that DEK3 is a chromatin architectural protein capable of modulating DNA topology, DNA accessibility, and gene expression. Furthermore, we show that functional levels of DEK3 are crucial for stress tolerance.

Our biochemical analyses showed that DEK3 binds to histones and associates to the chromatin in planta. DEK3 specifically copurified with histones H3 and H4. In far-Western blot analyses, DEK3 bound to H3 and H4 but not to H2A and H2B. Consistent with this direct binding study, DEK3 coimmunoprecipitated from plant extracts with histones H3 and H4 but not with histones H2A and H2B, indicating that DEK3 is not associated with fully assembled nucleosomes. DEK3 might interact with histones H3 and H4 before chromatin incorporation and/or DEK3 might associate with H3-H4 heterotetramers at the chromatin prior to their assembly with

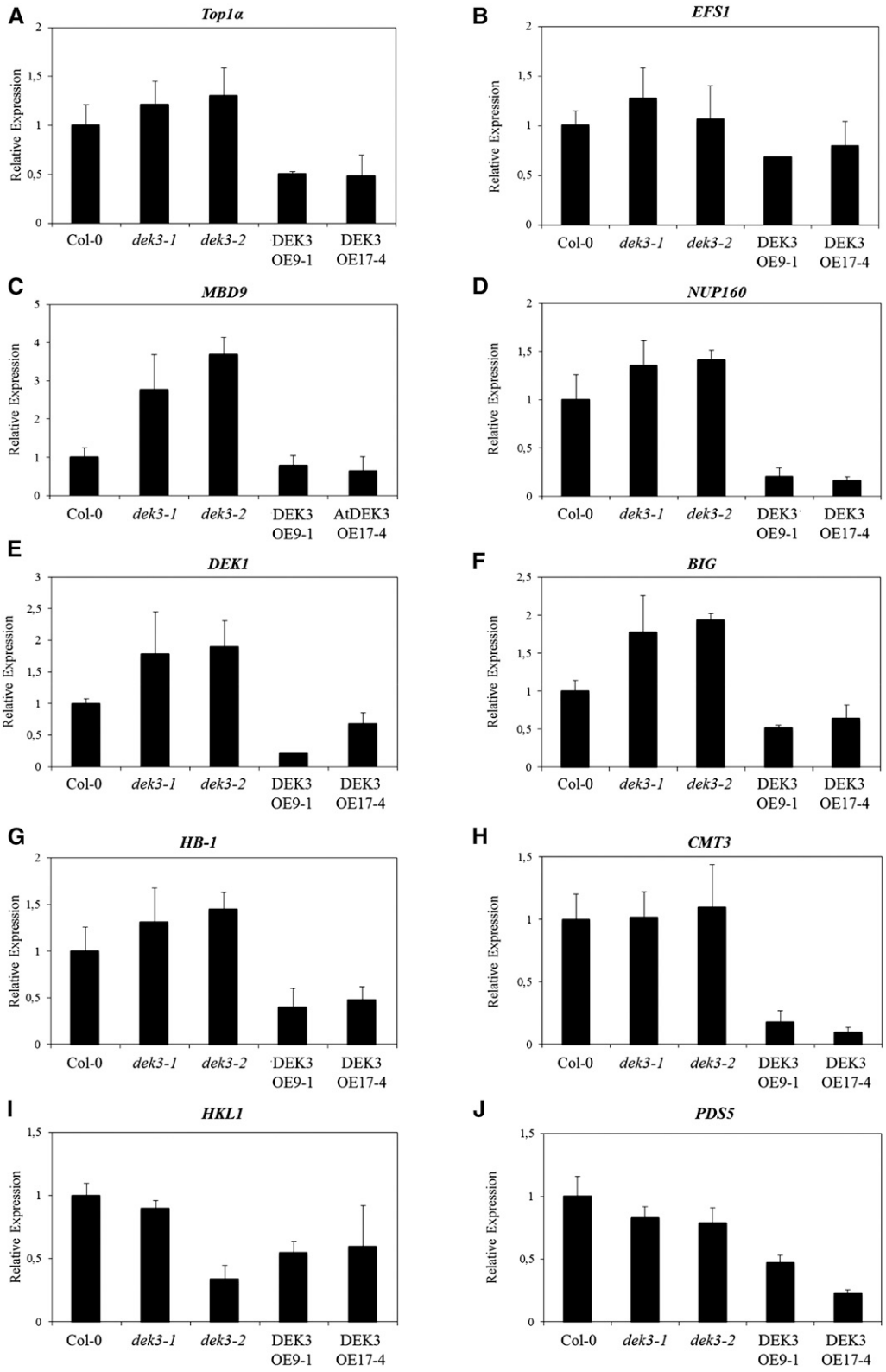

Figure 6. Influence of DEK3 on Locus-Specific Gene Expression.

histones H2A and H2B. Histone chaperones allow the ordered formation of nucleosome structure but are not a permanent component of the fully assembled nucleosome (Ransom et al., 2010; Elsässer and D'Arcy, 2013; Gurard-Levin et al., 2014). The specific binding of DEK3 to histones H3 and H4 and the influence of DEK3 levels on histone H3 occupancy and nucleosome density at DEK3 target sites in *Arabidopsis* are in line with recent biochemical analyses showing nucleosome assembly activity for Hs-DEK and Dm-DEK (Sawatsubashi et al., 2010; Kappes et al., 2011) and point toward a function of At-DEK3 as a plant H3-H4 histone chaperone, an interesting subject for future studies.

At-DEK3 carries two DNA binding domains: a DEK domain and a SAP box, a motif present in several chromatin-associated proteins involved in higher order chromatin structure (Kipp et al., 2000). Interestingly, At-DEK3 can change the topology of protein-free DNA in the presence of topoisomerase, indicating that At-DEK3 is able to induce local changes in DNA structure in a histone-independent manner. While the mechanism is still unknown, the ability of Hs-DEK to modify the structure of protein-free DNA appears to be mediated by its DNA binding and looping ability and not by inhibition of topoisomerase activity (Waldmann et al., 2002, 2003). At-DEK3 can form homodimers (Supplemental Figure 8) and likely heterodimers, as indicated by the coimmunopurification of DEK3 with DEK4 from *Arabidopsis* seedlings and the similar expression profile of *DEK3* and *DEK4* in different plant organs (Supplemental Figure 9). The results of the association studies with At-DEK proteins in vivo support previous in vitro and yeast two-hybrid data with Hs-DEK (Kappes et al., 2004a) and raise the possibility that DEK-DEK protein interaction induces DNA looping.

Identification of *Arabidopsis* DEK3-associated proteins in vivo indicates that DEK3 might be involved in tethering different proteins to the chromatin. Remarkably, we found DEK3 in association with proteins implicated in higher-order chromatin structure. DEK3 robustly associated with SCC3 and PDS5. SCC3 and PDS5 are regulatory subunits of the cohesin complex. Cohesin is an evolutionarily conserved, ring-shaped protein complex essential for a wide variety of intra- and intermolecular DNA processes and has important roles in sister chromatid cohesion, DNA repair, and gene regulation (Nasmyth and Haering, 2009; Wendt and Peters, 2009; Dorsett and Ström, 2012).

Interestingly, cohesin stabilizes chromatin loops (Hadjur et al., 2009; Mishiro et al., 2009; Nativio et al., 2009; Kagey et al., 2010; Degner et al., 2011; Seitan et al., 2011), and Hs-DEK was implicated in DNA looping by DEK-DEK protein interaction (Waldmann et al., 2003). Interaction of *Arabidopsis* DEK3 with DEK3 or with DEK4 proteins might promote DNA looping. Thus, one could envisage a scenario where DEK3 serves to bring two chromosome loci into close proximity, which are then entrapped within cohesin rings.

In line with a possible role of DEK3 in modulating chromatin architecture, we discovered the type IB topoisomerase Top1α as an in vivo interaction partner of DEK3. When a chromatin fiber undergoes a structural change, accompanying changes in its twist and writhe induce torsional stress. DNA topoisomerase I resolves topological problems associated with DNA replication, chromatin condensation, and transcription (Wang, 2002; Leppard and Champoux, 2005). We now provide evidence that DEK and topoisomerase I function together in an in vivo protein complex potentially modulating DNA structure.

It has been reported that Hs-DEK binds structured DNA (Waldmann et al., 2003). On the other hand, targeted binding assays indicated a specific location of DEK at different genes (Fu et al., 1997; Adams et al., 2003; Hu et al., 2005, 2007; Sammons et al., 2006). Our genome-wide binding studies with DEK3 in *Arabidopsis* revealed an enrichment of DEK3 at protein-coding genes over all chromosomes. The general binding profile of DEK3 showed an enrichment at gene bodies and their regulatory regions and a lower abundance of DEK3 in noncoding regions. This pattern is in line with a previous study based on immunofluorescence that indicated a favored binding of Hs-DEK to euchromatic regions (Hu et al., 2007).

Remarkably, At-DEK3 was enriched at three or more binding sites at its target genes. While the functional role of the overall At-DEK3 enrichment profile is presently unknown, the enrichment of At-DEK3 at the up- and downstream regulatory gene regions resembles that of histone H3.3 and RNA polymerase II in *Arabidopsis* and animals (Wollmann et al., 2012; Jin et al., 2009; Goldberg et al., 2010; Ooi et al., 2010; Ray-Gallet et al., 2011) and supports a possible role of At-DEK3 in transcriptional regulation.

Analysis of plants with altered DEK3 levels provide evidence that DEK3 contributes to transcriptional regulation as a repressor. DEK3 binding genes were downregulated in seedlings overexpressing DEK3. In *dek3* mutants, expression was generally moderately upregulated. The modest effect in *dek3* seedlings might be due to redundancy of DEK3 with other DEK isoforms (for transcript levels of all DEK family members in different plant organs, see Supplemental Figure 9) or indicate that, in addition to DEK3 depletion from the chromatin, other factors are needed to efficiently stimulate transcription of these genes.

In animal systems, DEK acts as a transcriptional inhibitor (Sammons et al., 2006; Gamble and Fisher, 2007; Kappes et al., 2011) or inducer (Campillos et al., 2003; Sawatsubashi et al., 2010). In our experimental system, DEK3 functioned as a repressor of, at least, a subset of DEK3 target genes. A role for DEK3 in gene repression is supported by the association of DEK3 with HDA3/HDT1. Histone deacetylases are critical for transcriptional repression (Haberland et al., 2009). It might thus be possible that recruitment of HDA3 by DEK3 promotes gene repression at DEK3 binding sites.

Figure 6. (continued).

Transcript levels of **(A)** *Top1*α, **(B)** *EFS1*, **(C)** *MBD9*, **(D)** *NUP160*, **(E)** *DEK1* (*Defective kernel 1*), **(F)** *BIG*/*ASA1*, **(G)** *HB-1*, **(H)** *CMT3*, **(I)** *HKL1*, and **(J)** *PDS5* were analyzed by RT-qPCR in Col-0, *dek3-1*, *dek3-2*, and DEK3-overexpressing (line 9-1 and line 17-4) *Arabidopsis* seedlings. Data are means ± relative SD of three technical measurements. Data from three biological replicas showed similar results.

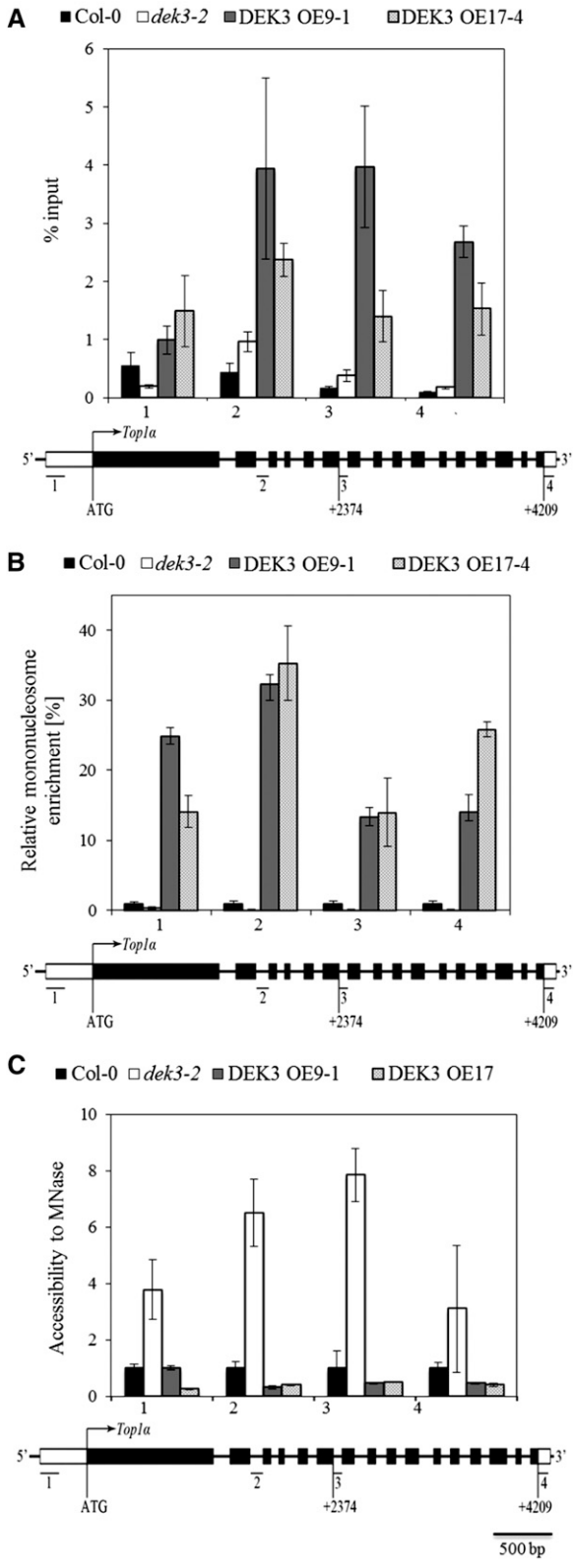

Figure 7. Influence of DEK3 Levels on Nucleosome Density at the *Top1*α Locus.

Important for transcriptional regulation, DEK3 levels affected in vivo nucleosome occupancy and DNA accessibility. Nucleosome density was increased in plants with elevated DEK3 levels, whereas nucleosome density at the *Top1*α and the *MBD9* loci was reduced in DEK3-deficient plants. Consistent with a function of DEK3 in chromatin compaction, nuclease accessibility of the *Top1*α and the *MBD9* loci was significantly increased in *dek3* mutants but decreased in DEK3-overexpressing plants. These in vivo data are in line and go beyond the observation that in vitro depletion or knockdown of DEK in human cells enhanced overall nuclease sensitivity (Gamble and Fisher, 2007; Kappes et al., 2011).

Altogether, DEK3 might contribute to transcriptional regulation through different mechanisms. DEK3 could have a regulatory effect on gene expression by altering DNA accessibility and/or by recruiting different chromatin and transcriptional regulators. Additionally, the potential of DEK3 to induce conformational changes in DNA and to modulate higher order chromatin structure might contribute to the highly complex process of gene regulation.

Chromatin organization plays a key role in stress responses (Kim et al., 2010; Zhu et al., 2012; Han and Wagner, 2014). In this work, we show that fine-tuned DEK3 levels are critical for salt stress tolerance. Salinity is a major stress for plants and has a severe effect on agricultural yield worldwide. *DEK3* was transcriptionally downregulated by salinity. Plants with constitutively elevated levels of DEK3 were significantly more sensitive to high salinity, whereas plants deficient in DEK3 were more tolerant to NaCl. It is tempting to speculate that *dek3* plants might be more tolerant to stress by keeping chromatin in a more open state and thus facilitating the access of stress-induced transcriptional regulators, while in DEK3 overexpression plants with higher nucleosome occupancy, accessibility to stress-induced regulators might be impeded by a more compact chromatin. Future studies will aim to investigate this hypothesis. DEK3 mutants also displayed an altered tolerance to heat stress (Supplemental Figure 10), showing that the regulatory function of DEK3 during the stress response is not restricted to salt stress and is likely more general.

(A) Histone H3 occupancy. ChIP assays using specific histone H3 antibodies were performed in Col-0, *dek3-2*, and DEK3 overexpressor lines 9-1 and 17-4, followed by qPCR for the indicated regions. Enrichment levels are represented relative to input.

(B) Nucleosome density. Following MNase I digestion, mononucleosomes were isolated from Col-0, *dek3-2*, and DEK3 overexpressor lines 9-1 and 17-4. Subsequently, qPCR was performed on the indicated regions. Relative mononucleosome enrichment levels were normalized to Col-0.

(C) MNase accessibility. CHART assays were performed using the accessibility agent MNase I and nuclei from Col-0, *dek3-2*, and DEK3 overexpressor lines 9-1 and 17-4. Genomic DNA was subsequently analyzed by qPCR. Data are depicted as fold change in DNA accessibility normalized to Col-0.

Schematic diagrams illustrate the *Top1*α genomic regions analyzed. Black and white rectangular boxes represent CDS and UTR, respectively. Data are means ± relative SD of three technical measurements and are representative of two independent biological experiments.

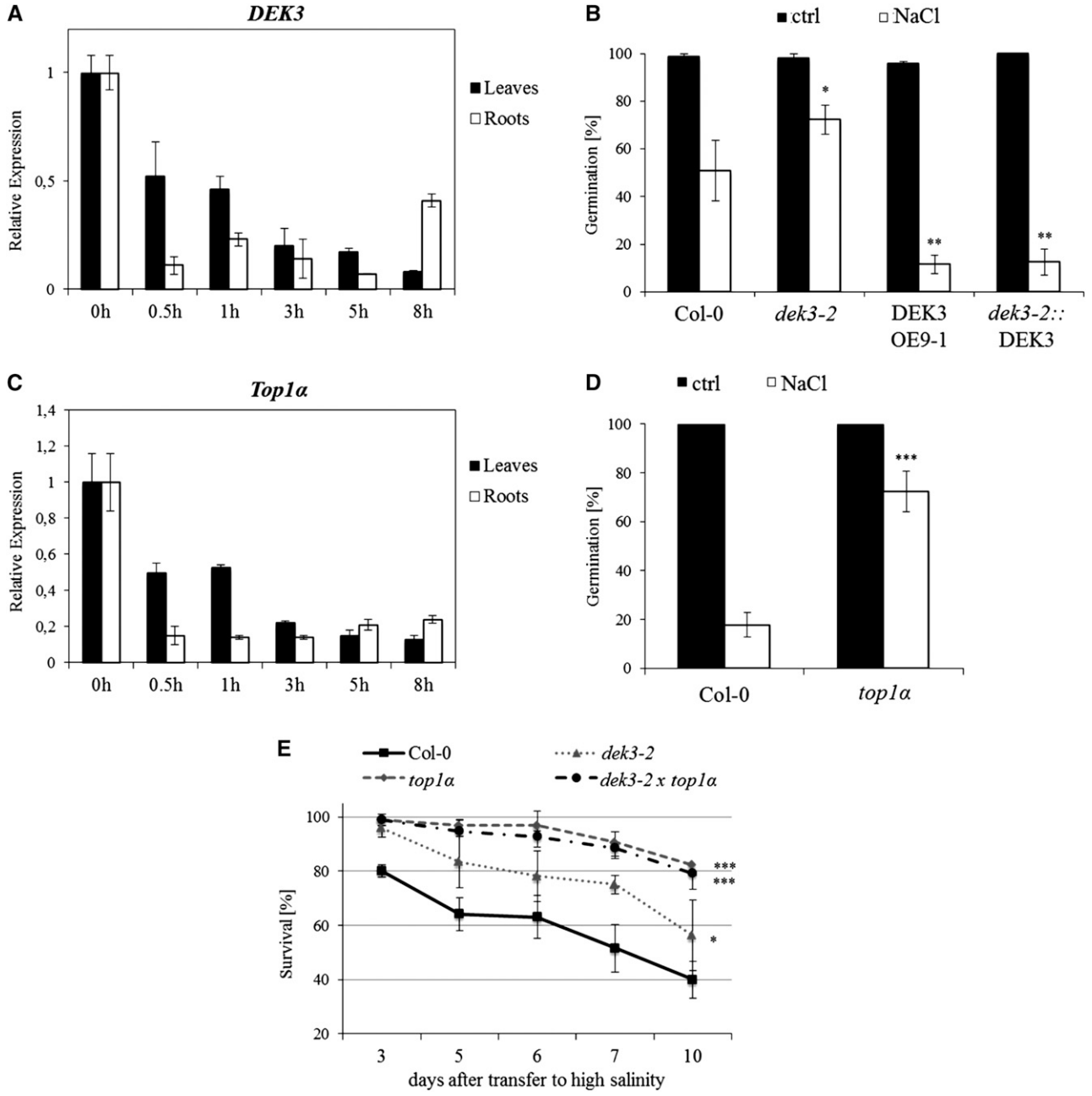

Figure 8. Involvement of DEK3 and Top1α in the *Arabidopsis* Salt Stress Response.

(A) and **(C)** *DEK3* and *Top1*α transcript levels are downregulated by salt stress. *DEK3* **(A)** and *Top1*α **(C)** expression in shoots and roots of plants in controls and under salt stress conditions was analyzed by RT-qPCR. Ten-day-old Col-0 seedlings were transferred to plates without (control) or with supplementation of 200 mM NaCl. Relative expression levels were normalized with respect to the controls. Data are means ± SD of three technical measurements. Data from three biological replicas showed similar results.

(B) and **(D)** DEK3 and Top1α regulate salt stress tolerance. Germination efficiency of wild-type Col-0, *dek3-2*, and DEK3-CFP overexpressors **(B)** and of *top1*α mutants **(D)** was analyzed on half-strength MS plates without and with supplementation of 200 mM NaCl. Data are means ± relative SD of three independent biological replicates with $n = 55$ (DEK3) and $n = 28$ (Top1α) for each genotype. Asterisks indicate a significant difference (*$P < 0.05$; **$P < 0.01$; ***$P < 0.001$) using one-way ANOVA for pairwise comparison to Col-0 under stress conditions.

(E) DEK3 and Top1α function in the same signaling pathway. Survival rate of Col-0, *dek3-2*, *top1*α, and *dek3-2 top1*α double knockout plants on medium supplemented with 200 mM NaCl. Data are means of four independent biological experiments with at least 24 plants each. Asterisks indicate a significant difference (*$P < 0.05$; ***$P < 0.001$) using one-way ANOVA for pairwise comparison to Col-0 under stress conditions.

Interestingly, DEK3 and TOP1α function in the same genetic pathway to modulate salt stress tolerance, extending biochemical data that DEK3 and Top1α interact in planta and have complementary roles in modulating DNA structural changes.

Virtually all DNA-dependent processes are determined by chromatin architecture. Identification of DEK3 as a plant chromatin protein that modulates chromatin accessibility opens new avenues for future studies on plant chromatin organization and regulation. The association of DEK3 with different proteins involved in diverse biological processes inherent to DNA, together with its ability to change DNA structure together with topoisomerase, indicate that DEK3 is a multifunctional chromatin-associated protein potentially involved in many cellular processes.

METHODS

Plant Growth and Stress Treatments

Arabidopsis thaliana ecotype Col-0 was germinated on half-strength Murashige and Skoog (MS) medium (Duchefa). After 10 d, seedlings were transferred to soil and cultivated in a 16-h-light/8-h-dark regime at 150 μmol m^{-2} s^{-1} light intensity and 60% relative humidity. For germination assays under high salt conditions, seeds were germinated on half-strength MS or half-strength MS supplemented with 200 mM NaCl. For gene expression analysis, seedlings grown on a mesh on liquid half-strength MS medium were transferred to either half-strength MS (control) or to medium supplemented with 200 mM NaCl for 0, 0.5, 1, 3, 5, and 8 h. Seeds used for one experiment were obtained from parental plants propagated in the same growth chamber at the same time.

Plant Material and Plasmid Constructs

The *dek3* mutants (*dek3-1*, SALK_054095.55.75.x; *dek3-2*, SALK_112581.46.05.x) were genotyped using primers AtDEK3_fw0 and AtDEK3_rev5, as well as AtDEK3_fw6 and AtDEK3_rev6 (Supplemental Table 2). The *top1α* mutant (SALK_112625.35.05.x) was genotyped using the primers Top1α_fw3 and Top1α_rev3 (Supplemental Table 2). The coding DNA sequence (CDS) of DEK3 was amplified by PCR using the primers AtDEK3_IF_fw and AtDEK3_IF_rev (Supplemental Table 2) and cloned with In-Fusion Advantage PCR cloning kit (#639638; Clontech) into the binary vector pGreenII0029 under the control of the 35S promoter. A CFP tag was cloned into the *Not*I site downstream of the coding sequence. Constructs were verified by sequencing. *Arabidopsis* Col-0 plants were transformed using the floral dip method (Clough and Bent, 1998).

Gene Expression Analysis

Total RNA was isolated from plant material using TRI Reagent (#9424; Sigma-Aldrich) and treated with RNase-free DNase (#EN0525; Thermo Scientific) following the manufacturer's protocol. For RT-qPCR, first-strand cDNA synthesis from 1 μg of total RNA was done using RevertAid H Minus First Stand cDNA Synthesis Kit (#K1632; Thermo Scientific). One microliter of cDNA was used for real-time PCR reactions using Sso Advanced (#172-5262; Bio-Rad) on an iQ5 multicolor real-time PCR detection system (Bio-Rad). All experiments were performed three times with independent RNA samples under the following cycling conditions: a 95°C hold for 10 min followed by 45 cycles at 95°C for 10 s, 55°C for 20 s, and 72°C for 30 s. Nonspecific PCR products were identified by dissociation curves. Relative expression values were calculated with the iQ5 Optical System Software 2.0 (Bio-Rad) according to Vandesompele et al. (2002). Primer efficiencies were calculated by relative standard curves. PP2A and Ubiquitin were used as normalization controls. Normalized gene expression was represented relative to wild-type controls. The primers were designed based on the 3′ UTR for DEK3 and Top1α (Supplemental Table 2).

Expression and Purification of Recombinant Protein

The coding sequence of DEK3 was amplified from cDNA by PCR using the primers AtDEK3_IF_fw and AtDEK3_IF_rev (Supplemental Table 2) and cloned with In-Fusion Advantage PCR cloning kit (#639650; Clontech) into pGEX-6P-1. Recombinant protein was expressed as GST fusion protein in *Escherichia coli* BL21 codon plus strain. Proteins were purified using the Sepharose beads affinity method (Glutathione Sepharose 4B, #17-0756-01; GE Healthcare).

Protein Extraction, Immunoblot Analysis, and Coimmunoprecipitation Analysis

Total proteins from *Arabidopsis* leaves or seedlings were extracted using Laemmli extraction buffer (100 mM Tris, pH 6.8, 100 mM DTT, 4% SDS, and 20% glycerol). Cytosolic extraction buffer (20 mM Tris, pH 8, 1 mM EDTA, 20 mM NaCl, 1 mM PMSF, 1 μg/mL leupeptin hemisulfate, 2 μg/mL pepstatin A, and 2 μg/mL aprotinin; all Sigma-Aldrich) was used to extract cytosolic proteins from *Arabidopsis* leaves or seedlings. Nuclear fractions for coimmunoprecipitation and immunoblot analysis were extracted as described for chromatin immunoprecipitation except that the material was not sheared. Protein concentration was assessed using Bradford method. Membranes were probed with a 1:1000 dilution of GFP antibodies (#11814460001; Roche), 1:3000 dilution H2A antibodies (#ab13923; abcam), H2B antibodies (#ab1790; abcam), H3 antibodies (#ab1791; abcam), H4 antibodies (#ab10158; abcam), or 1:1.1000 dilution of nitrate reductase antibodies (#AS08 310; Agrisera). Goat IRDye 800CW anti-mouse (#926-32210; LI-COR) or goat IRDye 800 CW anti-rabbit (#926-32211; LI-COR) was used (1:20,000) as secondary antibodies for GFP, histone, or nitrate reductase primary antibodies. The signals were detected using the Odyssey Imagine System (LI-COR).

Transient Transformation

Agrobacterium tumefaciens strain GV3101 transformed with the DEK3-CFP construct was grown for 2 d at 28°C in 5 mL Luria-Bertani (LB). The preculture was used to inoculate 25 mL LB and incubated for 4 h at 28°C. Cells were pelleted and resuspended in 30 mL LB supplemented with 100 μM acetosyringone. After 2 h, cells were resuspended in 30 mL of 5% sucrose and infiltrated in tobacco (*Nicotiana tabacum*) leaves. Subcellular localization was examined 4 d after transformation by confocal laser scanning microscopy (LSM 710 Zeiss spectral confocal microscope).

Far-Western Blot Analysis

Ten micrograms of core histones (#10223565001; Roche) was separated on a 15% SDS-PAGE and transferred to a membrane. Renaturation of the histones was done in PBST-0.05% Tween 20 (PBST-T) for 2 h at room temperature, and the membrane was blocked in PBS-BSA (PBS, 2% BSA, and 0.5% Nonidet P-40) for 2 h at room temperature. The membrane was incubated with recombinant GST-DEK3 or GST alone (100 ng/cm^2) in PBS-BSA for 2 h at room temperature. After washing with PBS-T, DEK3 binding was detected using GST antibodies (#27-4577-01; GE Healthcare), and donkey IRDye 680 anti-goat (#926-32224; LI-COR) was used (1:20,000) as secondary antibody. The signals were detected using the Odyssey Imagine System (LI-COR).

Chromatin Immunoprecipitation

Ten-day-old *Arabidopsis* seedlings were cross-linked with 1% (w/v) formaldehyde in buffer MC (10 mM KPO_4, pH 7, 50 mM NaCl, and 100 mM

sucrose) for 30 min. Formaldehyde was quenched for 15 min by adding glycine to a final concentration of 125 mM. Seedlings were washed twice with MC buffer and ground in liquid nitrogen. Five grams of ground powder was resuspended in 30 mL extraction buffer (2.5% [w/v] Ficoll 400, 5% [w/v] Dextran T40, 400 mM sucrose, 25 mM Tris, pH 7.5, and 10 mM $MgCl_2$) supplemented with protease inhibitor mix [1 mM PMSF, 1 μg/mL pepstatin A, 1 μg/mL leupeptin hemisulfate, 1 μg/mL aprotinin, 2.5 μg/mL *trans*-epoxysuccinyl-L-leucylamido(4-guanidino)butane (E64), 2 mM EGTA, and 1 μL/mL β-mercaptoethanol; all Sigma-Aldrich] and incubated for 30 min on ice. The homogenate was filtered through two layers of Miracloth and 0.5% Triton X-100 was added. After 15 min on ice, the cells were pelleted and resuspended in 2 mL extraction buffer supplemented with 0.1% Triton X-100. Cells were again pelleted and resuspended in 1 mL extraction buffer. Nuclei pellets were resuspended in sonication buffer (10 mM HEPES, pH 7.4, and 1 mM EDTA) supplemented with 0.5% SDS and protease inhibitors and incubated for 30 min at 4°C on the turning wheel. Chromatin was sheared with a Bioruptor (high intensity, 60 min, 30-s/30-s intervals) to an average size less than 500 bp, as verified on a 1.5% agarose gel.

Precleared extracts from 500 μg protein were agitated overnight at 4°C with 2 μL GFP antibodies (#ab290; abcam) or 1 μL histone H3 antibodies (#ab1791; abcam) and 30 μL protein A sepharose 6 MB beads (#17-0469-01; GE Healthcare). Immunoprecipitates were washed three times with RIPA buffer (50 mM HEPES, pH 7.4, 140 mM NaCl, 1 mM EDTA, and 0.1% sodium deoxycholate) supplemented with 0.5% Tween 20, twice with RIPA buffer supplemented with 0.5% TritonX-100 and then eluted with 100 μL ice-cold glycine buffer (100 mM glycine, pH 2.8, 500 mM NaCl, and 0.05% Tween 20). Eluates were neutralized with 50 μL of 1 M Tris, pH 9. After incubation with 10 μg/μL proteinase K (#03115887001; Roche), overnight cross-links were reversed for 8 h at 65°C. ChIP DNA was treated with 100 μg/μL RNase A (#EN0531; Thermo Scientific), purified by phenol:chloroform:isoamylalcohol extraction, and precipitated with 0.1 volumes of 3 M sodium acetate and 2 volumes of 100% ethanol. ChIP DNA was resuspended in 30 μL TE buffer.

Construction and Sequencing of Illumina Libraries

Library preparation and sequencing was performed by the Campus Service Support Facilities in Vienna. The libraries were constructed using KAPA Library Preparation Kit Illumina series (#KK8201; KAPA Biosystems). To summarize, 5 to 10 ng DNA was end-repaired, A bases were added to the 3′ end of the DNA fragments, and adapters were ligated. After each of these steps, the DNA was purified using the Qiagen MiniElute PCR purification kit. DNA was size-selected on a 2% agarose gel and purified using Qiagen Gel Extraction and MiniElute PCR purification kit. DNA was PCR amplified using a program of (1) 30 s at 98°C, (2) 15 cycles of 40 s at 98°C, 30 s at 65°C, and 30 s at 72°C, and (3) a 5-min extension at 72°C. The final libraries were purified using a Qiagen MiniElute PCR purification kit. The libraries were validated using an Agilent Bioanalyzer, and DNA concentration was determined by qPCR. Library DNA was captured on an Illumina flow cell for cluster generation, and 36-bp single-end sequencing was achieved on a Genome Analyzer IIx (Illumina) following Illumina's protocol. Each library was sequenced in one lane of the flow cell.

Sequencing Data Analysis

Sequenced reads were aligned with mismatch cost set to 1 and limit to 7 using CLC Genomics Workbench 7.0. As reference genome, TAIR10 was used. Significant binding regions were identified using CLC Genomics Workbench 7.0 with the following settings: window size, 150 nucleotides; maximum false discovery rate, 5%; shift reads based on fragment length, 300 nucleotides. False discovery rate was determined according to Ji et al. (2008). Peak boundaries were refined and candidate peaks were filtered using two filtering criteria: based on difference in read orientation count 0.4 and on probability of identical locations of forward and reverse reads 0.1. This ensured that peaks were only called if there was a well-balanced number of forward and reverse reads. Background peaks were filtered using a similar-sized data set of uniquely mapped reads obtained from sequencing the input DNA. Reads were normalized according to the CLC manual (http://www.clcsupport.com/clcgenomicsworkbench/650/index.php?manual=Peak_finding_false_discovery_rates.html). Peaks were annotated based on the location of their summits with respect to nearby genes, as annotated in TAIR10 by the following criteria: If a peak summit was located in (1) a gene's exon, (2) a gene's intron, (3) in the 5′ UTR (upstream 1000 bp from the start codon), (4) in the 3′ UTR (downstream 1000 bp from the stop codon), or (5) binding sites not selected by the above four criteria were defined as the binding sites in the intergenic regions.

Data-mining and cross experiment data integration were performed using MySQL open-source relational database management system and custom SQL scripts. TAIR10 was used as index in order to match peaks in the same gene between different samples. Finally, precise genomic coordinates of peaks were used to verify the identity of the peaks. To identify robust DEK3 DNA binding sites, we determined peaks shared by the three independent DEK3-CFP transgenic lines.

To determine the genomic distribution of DEK3 peaks relative to the gene structure, gene loci were divided into regions 1, 2, and 3 kb upstream of the translational start site (ATG), a region from the ATG to the stop codon, and into regions 1 and 2 kb downstream of the stop codon. Taking the length of the gene into account, we calculated the relative position of each peak summit between start and stop codon, as well as in the 5′ and 3′ flanking regions, using the number of reads under each peak summit. Subsequently, these data were averaged across all DEK3 target genes and normalized to the total number of reads and peaks. Peaks outside these regions were not included in the analysis.

Gene Ontology term classification was performed with Babelomics (http://babelomics.bioinfo.cipf.es).

ChIP-qPCR

To validate genes identified by ChIP-Seq, ChIP products from three independent biological samples from three independent DEK3-CFP lines were used to perform qPCR. Data from three technical replicates were collected under the following cycling conditions: a 95°C hold for 10 min followed by 45 cycles at 95°C for 10 s, 55°C for 20 s, and 72°C for 30 s. Nonspecific PCR products were identified by dissociation curves. The immunoprecipitation signal was calculated relative to the input signal. Primers are listed in Supplemental Table 2.

Analysis of Protein Association by Mass Spectrometry

Immunoprecipitations were performed using the same conditions as for ChIP experiments except that the material was not sheared and the antibodies were cross-linked to the beads using 20 mM dimethyl pimelimidate dihydrochloride (Sigma-Aldrich). After immunoprecipitation, beads were washed five times with RIPA buffer supplemented with 0.5% Tween 20, 10 times with immunoprecipitation buffer (20 mM Tris, pH 7.5, 150 mM NaCl, 2 mM EDTA, and 10% glycerol) and twice with 150 mM NaCl. Proteins were eluted with 100 mM glycine, pH 2.0, and neutralized with 1.5 M Tris, pH 9.2. Eluates were reduced, alkylated, and digested using trypsin (#V5280; Promega).

Samples were subjected to nanoflow chromatography using an UltiMate 3000 HPLC RSLC nano system (Thermo Fisher Scientific) prior to introduction into a mass spectrometer for further analysis. Mass spectrometry was performed on an LTQ Orbitrap Velos mass spectrometer (Thermo Fisher Scientific), equipped with a Proxeon nanospray source. Peptides were loaded onto a trap column (Thermo Fisher Scientific) at a flow rate of 25 μL min^{-1} using 0.1% trifluoroacetic acid as mobile phase. After 10 min, the trap column was switched to analytic column (Thermo Fisher Scientific). Peptides were eluted using a flow rate or 230 nL min^{-1} and a binary 2-h gradient for 165 min.

For peptide identification, the ".RAW-files" were loaded into Proteome Discoverer (Thermo Fisher Scientific), and MS/MS spectra were searched using Mascot (Matrix Science) against the NCBI *Arabidopsis* non-redundant protein sequence database. The following search parameters were used: β-methylthiolation on cysteine was set as a fixed modification, oxidation on methionine, substitution of glutamine against pyro-glutamic acid, and phosphorylation on serine, threonine and tyrosine were set as variable modifications. Monoisotopic masses were searched within unrestricted protein masses for tryptic peptides. The peptide mass tolerance was set to ±5 ppm and the fragment mass tolerance to ±0.5 D. The maximal number of missed cleavages was set to 2. For better visualization, the results of the searches were loaded into Scaffold (Proteome Software) using a minimum of two unique peptides per protein and a Mascot Score of at least 20 as cutoff filters.

DNA Topology Assay

DNA topology assays were performed as described by Waldmann et al. (2002) with small modifications. Purified recombinant DEK protein was dialyzed with Whatman filters (type: 0.025 μm VSWP) against topoisomerase buffer (50 mM Tris, pH 7.5, 50 mM NaCl, 0.1 mM EDTA, 1 mM DTT, and 20% glycerol) in the presence of 1 μg of BSA per μL for 90 min at 4°C. One hundred nanograms of plasmid DNA (pBluescript) was incubated with GST-DEK3 or GST alone in the presence of 1 unit of topoisomerase I (#M2852; Promega). The reactions were performed in the topoisomerase buffer in a total volume of 90 μL for 60 min at 37°C. After proteinase K (#03115887001; Roche) digestion, DNA was precipitated and analyzed on a 0.8% agarose gel in 0.5× TBE (45 mM Tris-borate and 1 mM EDTA) at 2 V/cm for 16 h. The gel was stained with SYBR Green I (#S9430; Sigma-Aldrich).

Histone H3 Occupancy

For analysis histone H3 occupancy, ChIP and qPCR was performed as described above.

Isolation of Mononucleosomes and qPCR

Nuclei were extracted as mentioned above, resuspended in 500 μL MNase buffer (50 mM Tris, pH 8.0, and 5 mM $CaCl_2$) and incubated for 5 min at 37°C with 75 units of MNase I (#2910A; TaKaRa). The reaction was stopped with 50 mM EDTA for 45 min at 65°C. DNA was purified by phenol:chloroform:isoamylalcohol extraction and precipitated with 0.1 volumes of 3 M sodium acetate and 2 volumes of 100% ethanol. DNA was resuspended in 20 μL TE buffer and separated in 2% (w/v) agarose gels. From these gels, the ~150-bp band was precisely excised, and mononucleosomal DNA was purified using the Wizard SV gel clean-up system (#A9282; Promega). DNA was quantified by qPCR as described above using primers spanning <150 bp.

CHART-PCR

Accessibility of DNA to digestion with MNase was analyzed with CHART-PCR as described previously (Rao et al., 2001; Sutcliffe et al., 2009) with small modifications. Nuclei were extracted as mentioned above and resuspended in 500 μL MNase buffer (50 mM Tris, pH 8.0, and 5 mM $CaCl_2$). Nuclei were incubated for 15 min at 37°C with 15 units of MNase I (#2910A; TaKaRa). The reaction was stopped with 50 mM EDTA for 45 min at 65°C. DNA was purified by phenol:chloroform:isoamylalcohol extraction and precipitated with 0.1 volumes of 3 M sodium acetate and 2 volumes of 100% ethanol. DNA was resuspended in 20 μL TE buffer. DNA was quantified by qPCR as described above using primers spanning more than 150 bp. For MNase accessibility, the percentage of cutting was calculated by expressing the amount of genomic DNA remaining as a percentage of the amount of genomic DNA in cells that were not treated with MNase.

Data Availability

The ChIP-Seq data from this publication were submitted to the Gene Expression Omnibus (http://www.ncbi.nlm.nih.gov/geo/) database (accession number GSE55893). The protein interactions from this publication have been submitted to the IMEx (Orchard et al., 2012) consortium and assigned the identifier IM-22255.

Accession Numbers

Sequence data from this article can be found in the Arabidopsis Genome Initiative under the following accession numbers: *DEK3*, At4g26630; *Top1α*, At5g55300; *EFS1*, At1g77300; *CMT3*, At1g69770; *DEK1* (*Defective kernel 1*), At1g55350; *NUP160*, At1g33410; *PDS5*, At5g47690; *HKL1*, At1g50460; *MBD9*, At3g01460; *HB-1*, At1g28420; *BIG*, At3g02260; *PP2A*, At1g69770; *Ubiquitin*, At2g35360; *PIP5K1*, At1g21980; *DEK1*, At3g48710; *DEK2*, At5g63550; and *DEK4*, At5g55660.

Supplemental Data

The following materials are available in the online version of this article.

Supplemental Figure 1. Expression of *DEK3* and Characterization of *dek3* T-DNA Insertion Mutants and DEK3 Overexpressor Lines.

Supplemental Figure 2. Overview of Genes Associated with DEK3 Binding Sites.

Supplemental Figure 3. ChIP-qPCR Verification of Specific DEK3 Binding Sites.

Supplemental Figure 4. ChIP-qPCR of Wild-Type Control.

Supplemental Figure 5. Influence of DEK3 Levels on Nucleosome Density at the *MBD9* Locus.

Supplemental Figure 6. Influence of DEK3 Levels on Nucleosome Density at the *PIPK1* Control Locus.

Supplemental Figure 7. Characterization of *top1α* T-DNA Insertion Mutant and Top1α Expression Pattern.

Supplemental Figure 8. DEK3 Interaction with DEK3.

Supplemental Figure 9. Expression of *DEK* Family Members.

Supplemental Figure 10. Involvement of DEK3 in the *Arabidopsis* Heat Stress Response.

Supplemental Table 1. Read Counts, Number of Peaks, and Number of Target Genes Identified by ChIP-Seq.

Supplemental Table 2. List of Primers.

Supplemental Data Set 1. Identified DEK3 Binding Sites.

ACKNOWLEDGMENTS

We thank O. Mittelsten Scheid for discussions and comments on the article, F. Kappes and T. Waldmann for discussions, A. Auer and B. Dekrout for technical assistance, and M. Grelon for SSC3 antibodies. The work was supported by the Austrian Science Foundation (Grant P 22062-B16) and by FP7 ITN 215174.

AUTHOR CONTRIBUTIONS

S.W. designed and performed the experiments. B.K. and S.W. did sequencing data analyses. K.M. performed the mass spectrometry. J.M. performed *top1α* stress assays. C.J. and S.W. analyzed the data and prepared the article.

Received June 26, 2014; revised October 1, 2014; accepted October 22, 2014; published November 11, 2014.

REFERENCES

Adams, B.S., Cha, H.C., Cleary, J., Haiying, T., Wang, H., Sitwala, K., and Markovitz, D.M. (2003). DEK binding to class II MHC Y-box sequences is gene- and allele-specific. Arthritis Res. Ther. **5:** R226–R233.

Alexiadis, V., Waldmann, T., Andersen, J., Mann, M., Knippers, R., and Gruss, C. (2000). The protein encoded by the proto-oncogene DEK changes the topology of chromatin and reduces the efficiency of DNA replication in a chromatin-specific manner. Genes Dev. **14:** 1308–1312.

Aravind, L., and Koonin, E.V. (2000). SAP - a putative DNA-binding motif involved in chromosomal organization. Trends Biochem. Sci. **25:** 112–114.

Babaei-Jadidi, R., et al. (2011). FBXW7 influences murine intestinal homeostasis and cancer, targeting Notch, Jun, and DEK for degradation. J. Exp. Med. **208:** 295–312.

Broxmeyer, H.E., Kappes, F., Mor-Vaknin, N., Legendre, M., Kinzfogl, J., Cooper, S., Hangoc, G., and Markovitz, D.M. (2012). DEK regulates hematopoietic stem engraftment and progenitor cell proliferation. Stem Cells Dev. **21:** 1449–1454.

Broxmeyer, H.E., Mor-Vaknin, N., Kappes, F., Legendre, M., Saha, A.K., Ou, X., O'Leary, H., Capitano, M., Cooper, S., and Markovitz, D.M. (2013). Concise review: role of DEK in stem/progenitor cell biology. Stem Cells **31:** 1447–1453.

Campillos, M., García, M.A., Valdivieso, F., and Vázquez, J. (2003). Transcriptional activation by AP-2alpha is modulated by the oncogene DEK. Nucleic Acids Res. **31:** 1571–1575.

Chelysheva, L., et al. (2005). AtREC8 and AtSCC3 are essential to the monopolar orientation of the kinetochores during meiosis. J. Cell Sci. **118:** 4621–4632.

Clough, S.J., and Bent, A.F. (1998). Floral dip: a simplified method for Agrobacterium-mediated transformation of *Arabidopsis thaliana*. Plant J. **16:** 735–743.

Degner, S.C., et al. (2011). CCCTC-binding factor (CTCF) and cohesin influence the genomic architecture of the Igh locus and antisense transcription in pro-B cells. Proc. Natl. Acad. Sci. USA **108:** 9566–9571.

Dorsett, D., and Ström, L. (2012). The ancient and evolving roles of cohesin in gene expression and DNA repair. Curr. Biol. **22:** R240–R250.

Doskočilová, A., Kohoutová, L., Volc, J., Kourová, H., Benada, O., Chumová, J., Plíhal, O., Petrovská, B., Halada, P., Bögre, L., and Binarová, P. (2013). NITRILASE1 regulates the exit from proliferation, genome stability and plant development. New Phytol. **198:** 685–698.

Du, J., Huang, Y.P., Xi, J., Cao, M.J., Ni, W.S., Chen, X., Zhu, J.K., Oliver, D.J., and Xiang, C.B. (2008). Functional gene-mining for salt-tolerance genes with the power of Arabidopsis. Plant J. **56:** 653–664.

Edgar, R.C., and Batzoglou, S. (2006). Multiple sequence alignment. Curr. Opin. Struct. Biol. **16:** 368–373.

Elsässer, S.J., and D'Arcy, S. (2013). Towards a mechanism for histone chaperones. Biochim. Biophys. Acta **1819:** 211–221.

Faulkner, N.E., Hilfinger, J.M., and Markovitz, D.M. (2001). Protein phosphatase 2A activates the HIV-2 promoter through enhancer elements that include the pets site. J. Biol. Chem. **276:** 25804–25812.

Fu, G.K., Grosveld, G., and Markovitz, D.M. (1997). DEK, an autoantigen involved in a chromosomal translocation in acute myelogenous leukemia, binds to the HIV-2 enhancer. Proc. Natl. Acad. Sci. USA **94:** 1811–1815.

Gamble, M.J., and Fisher, R.P. (2007). SET and PARP1 remove DEK from chromatin to permit access by the transcription machinery. Nat. Struct. Mol. Biol. **14:** 548–555.

Gentry, M., and Hennig, L. (2014). Remodelling chromatin to shape development of plants. Exp. Cell Res. **321:** 40–46.

Goldberg, A.D., et al. (2010). Distinct factors control histone variant H3.3 localization at specific genomic regions. Cell **140:** 678–691.

Graf, P., Dolzblasz, A., Würschum, T., Lenhard, M., Pfreundt, U., and Laux, T. (2010). MGOUN1 encodes an Arabidopsis type IB DNA topoisomerase required in stem cell regulation and to maintain developmentally regulated gene silencing. Plant Cell **22:** 716–728.

Gurard-Levin, Z.A., Quivy, J.P., and Almouzni, G. (2014). Histone chaperones: assisting histone traffic and nucleosome dynamics. Annu. Rev. Biochem. **83:** 487–517.

Haberland, M., Montgomery, R.L., and Olson, E.N. (2009). The many roles of histone deacetylases in development and physiology: implications for disease and therapy. Nat. Rev. Genet. **10:** 32–42.

Hadjur, S., Williams, L.M., Ryan, N.K., Cobb, B.S., Sexton, T., Fraser, P., Fisher, A.G., and Merkenschlager, M. (2009). Cohesins form chromosomal cis-interactions at the developmentally regulated IFNG locus. Nature **460:** 410–413.

Han, S.K., and Wagner, D. (2014). Role of chromatin in water stress responses in plants. J. Exp. Bot. **65:** 2785–2799

Ho, L., and Crabtree, G.R. (2010). Chromatin remodelling during development. Nature **463:** 474–484.

Hollenbach, A.D., McPherson, C.J., Mientjes, E.J., Iyengar, R., and Grosveld, G. (2002). Daxx and histone deacetylase II associate with chromatin through an interaction with core histones and the chromatin-associated protein Dek. J. Cell Sci. **115:** 3319–3330.

Hu, H.G., Illges, H., Gruss, C., and Knippers, R. (2005). Distribution of the chromatin protein DEK distinguishes active and inactive CD21/CR2 gene in pre- and mature B lymphocytes. Int. Immunol. **17:** 789–796.

Hu, H.G., Scholten, I., Gruss, C., and Knippers, R. (2007). The distribution of the DEK protein in mammalian chromatin. Biochem. Biophys. Res. Commun. **358:** 1008–1014.

Ji, H., Jiang, H., Ma, W., Johnson, D.S., Myers, R.M., and Wong, W.H. (2008). An integrated software system for analyzing ChIP-chip and ChIP-seq data. Nat. Biotechnol. **26:** 1293–1300.

Jin, C., Zang, C., Wei, G., Cui, K., Peng, W., Zhao, K., and Felsenfeld, G. (2009). H3.3/H2A.Z double variant-containing nucleosomes mark "nucleosome-free regions" of active promoters and other regulatory regions. Nat. Genet. **41:** 941–945.

Kagey, M.H., et al. (2010). Mediator and cohesin connect gene expression and chromatin architecture. Nature **467:** 430–435.

Kappes, F., Scholten, I., Richter, N., Gruss, C., and Waldmann, T. (2004a). Functional domains of the ubiquitous chromatin protein DEK. Mol. Cell. Biol. **24:** 6000–6010.

Kappes, F., Damoc, C., Knippers, R., Przybylski, M., Pinna, L.A., and Gruss, C. (2004b). Phosphorylation by protein kinase CK2 changes the DNA binding properties of the human chromatin protein DEK. Mol. Cell. Biol. **24:** 6011–6020.

Kappes, F., Fahrer, J., Khodadoust, M.S., Tabbert, A., Strasser, C., Mor-Vaknin, N., Moreno-Villanueva, M., Bürkle, A., Markovitz, D.M., and Ferrando-May, E. (2008). DEK is a poly(ADP-ribose) acceptor in apoptosis and mediates resistance to genotoxic stress. Mol. Cell. Biol. **28:** 3245–3257.

Kappes, F., Waldmann, T., Mathew, V., Yu, J., Zhang, L., Khodadoust, M.S., Chinnaiyan, A.M., Luger, K., Erhardt, S., Schneider, R., and Markovitz, D.M. (2011). The DEK oncoprotein is a Su(var) that is essential to heterochromatin integrity. Genes Dev. **25:** 673–678.

Kavanaugh, G.M., et al. (2011). The human DEK oncogene regulates DNA damage response signaling and repair. Nucleic Acids Res. **39:** 7465–7476.

Kieber, J.J., Tissier, A.F., and Signer, E.R. (1992). Cloning and characterization of an *Arabidopsis thaliana* topoisomerase I gene. Plant Physiol. **99:** 1493–1501.

Kim, J.M., To, T.K., Nishioka, T., and Seki, M. (2010). Chromatin regulation functions in plant abiotic stress responses. Plant Cell Environ. **33:** 604–611.

Kipp, M., Göhring, F., Ostendorp, T., van Drunen, C.M., van Driel, R., Przybylski, M., and Fackelmayer, F.O. (2000). SAF-Box, a conserved protein domain that specifically recognizes scaffold attachment region DNA. Mol. Cell. Biol. **20:** 7480–7489.

Kreps, J.A., Wu, Y., Chang, H.S., Zhu, T., Wang, X., and Harper, J.F. (2002). Transcriptome changes for Arabidopsis in response to salt, osmotic, and cold stress. Plant Physiol. **130:** 2129–2141.

Kurkela, S., and Borg-Franck, M. (1992). Structure and expression of kin2, one of two cold- and ABA-induced genes of *Arabidopsis thaliana*. Plant Mol. Biol. **19:** 689–692.

Lawson, M.J., and Zhang, L. (2006). Distinct patterns of SSR distribution in the *Arabidopsis thaliana* and rice genomes. Genome Biol. **7:** R14.

Le Hir, H., Izaurralde, E., Maquat, L.E., and Moore, M.J. (2000). The spliceosome deposits multiple proteins 20-24 nucleotides upstream of mRNA exon-exon junctions. EMBO J. **19:** 6860–6869.

Le Hir, H., Gatfield, D., Izaurralde, E., and Moore, M.J. (2001). The exon-exon junction complex provides a binding platform for factors involved in mRNA export and nonsense-mediated mRNA decay. EMBO J. **20:** 4987–4997.

Leppard, J.B., and Champoux, J.J. (2005). Human DNA topoisomerase I: relaxation, roles, and damage control. Chromosoma **114:** 75–85.

Li, G., and Reinberg, D. (2011). Chromatin higher-order structures and gene regulation. Curr. Opin. Genet. Dev. **21:** 175–186.

Luger, K., Dechassa, M.L., and Tremethick, D.J. (2012). New insights into nucleosome and chromatin structure: an ordered state or a disordered affair? Nat. Rev. Mol. Cell Biol. **13:** 436–447.

McGarvey, T., Rosonina, E., McCracken, S., Li, Q., Arnaout, R., Mientjes, E., Nickerson, J.A., Awrey, D., Greenblatt, J., Grosveld, G., and Blencowe, B.J. (2000). The acute myeloid leukemia-associated protein, DEK, forms a splicing-dependent interaction with exon-product complexes. J. Cell Biol. **150:** 309–320.

Mishiro, T., Ishihara, K., Hino, S., Tsutsumi, S., Aburatani, H., Shirahige, K., Kinoshita, Y., and Nakao, M. (2009). Architectural roles of multiple chromatin insulators at the human apolipoprotein gene cluster. EMBO J. **28:** 1234–1245.

Müssig, C., Kauschmann, A., Clouse, S.D., and Altmann, T. (2000). The Arabidopsis PHD-finger protein SHL is required for proper development and fertility. Mol. Gen. Genet. **264:** 363–370.

Nasmyth, K., and Haering, C.H. (2009). Cohesin: its roles and mechanisms. Annu. Rev. Genet. **43:** 525–558.

Nativio, R., Wendt, K.S., Ito, Y., Huddleston, J.E., Uribe-Lewis, S., Woodfine, K., Krueger, C., Reik, W., Peters, J.M., and Murrell, A. (2009). Cohesin is required for higher-order chromatin conformation at the imprinted IGF2-H19 locus. PLoS Genet. **5:** e1000739.

Ooi, S.L., Henikoff, J.G., and Henikoff, S. (2010). A native chromatin purification system for epigenomic profiling in *Caenorhabditis elegans*. Nucleic Acids Res. **38:** e26.

Orchard, S., et al. (2012). Protein interaction data curation: the International Molecular Exchange (IMEx) consortium. Nat. Methods **9:** 345–350.

Pendle, A.F., Clark, G.P., Boon, R., Lewandowska, D., Lam, Y.W., Andersen, J., Mann, M., Lamond, A.I., Brown, J.W., and Shaw, P.J. (2005). Proteomic analysis of the Arabidopsis nucleolus suggests novel nucleolar functions. Mol. Biol. Cell **16:** 260–269.

Privette Vinnedge, L.M., Kappes, F., Nassar, N., and Wells, S.I. (2013). Stacking the DEK: from chromatin topology to cancer stem cells. Cell Cycle **12:** 51–66.

Punta, M., et al. (2012). The Pfam protein families database. Nucleic Acids Res. **40:** D290–D301.

Ransom, M., Dennehey, B.K., and Tyler, J.K. (2010). Chaperoning histones during DNA replication and repair. Cell **140:** 183–195.

Rao, S., Procko, E., and Shannon, M.F. (2001). Chromatin remodeling, measured by a novel real-time polymerase chain reaction assay, across the proximal promoter region of the IL-2 gene. J. Immunol. **167:** 4494–4503.

Ray-Gallet, D., Woolfe, A., Vassias, I., Pellentz, C., Lacoste, N., Puri, A., Schultz, D.C., Pchelintsev, N.A., Adams, P.D., Jansen, L.E.T., and Almouzni, G. (2011). Dynamics of histone H3 deposition in vivo reveal a nucleosome gap-filling mechanism for H3.3 to maintain chromatin integrity. Mol. Cell **44:** 928–941.

Riveiro-Falkenbach, E., and Soengas, M.S. (2010). Control of tumorigenesis and chemoresistance by the DEK oncogene. Clin. Cancer Res. **16:** 2932–2938.

Sammons, M., Wan, S.S., Vogel, N.L., Mientjes, E.J., Grosveld, G., and Ashburner, B.P. (2006). Negative regulation of the RelA/p65 transactivation function by the product of the DEK proto-oncogene. J. Biol. Chem. **281:** 26802–26812.

Sawatsubashi, S., et al. (2010). A histone chaperone, DEK, transcriptionally coactivates a nuclear receptor. Genes Dev. **24:** 159–170.

Schubert, V., Weissleder, A., Ali, H., Fuchs, J., Lermontova, I., Meister, A., and Schubert, I. (2009). Cohesin gene defects may impair sister chromatid alignment and genome stability in *Arabidopsis thaliana*. Chromosoma **118:** 591–605.

Seitan, V.C., et al. (2011). A role for cohesin in T-cell-receptor rearrangement and thymocyte differentiation. Nature **476:** 467–471.

Soares, L.M., Zanier, K., Mackereth, C., Sattler, M., and Valcárcel, J. (2006). Intron removal requires proofreading of U2AF/3′ splice site recognition by DEK. Science **312:** 1961–1965.

Soekarman, D., von Lindern, M., Daenen, S., de Jong, B., Fonatsch, C., Heinze, B., Bartram, C., Hagemeijer, A., and Grosveld, G. (1992). The translocation (6;9) (p23;q34) shows consistent rearrangement of two genes and defines a myeloproliferative disorder with specific clinical features. Blood **79:** 2990–2997.

Sutcliffe, E.L., Parish, I.A., He, Y.Q., Juelich, T., Tierney, M.L., Rangasamy, D., Milburn, P.J., Parish, C.R., Tremethick, D.J., and Rao, S. (2009). Dynamic histone variant exchange accompanies gene induction in T cells. Mol. Cell. Biol. **29:** 1972–1986.

Tabbert, A., Kappes, F., Knippers, R., Kellermann, J., Lottspeich, F., and Ferrando-May, E. (2006). Hypophosphorylation of the architectural chromatin protein DEK in death-receptor-induced apoptosis revealed by the isotope coded protein label proteomic platform. Proteomics **6:** 5758–5772.

Takahashi, T., Matsuhara, S., Abe, M., and Komeda, Y. (2002). Disruption of a DNA topoisomerase I gene affects morphogenesis in Arabidopsis. Plant Cell **14:** 2085–2093.

van Zanten, M., Tessadori, F., Peeters, A.J., and Fransz, P. (2012). Shedding light on large-scale chromatin reorganization in Arabidopsis thaliana. Mol. Plant **5:** 583–590.

Vandesompele, J., De Preter, K., Pattyn, F., Poppe, B., Van Roy, N., De Paepe, A., and Speleman, F. (2002). Accurate normalization of real-time quantitative RT-PCR data by geometric averaging of multiple internal control genes. Genome Biol **3:** RESEARCH0034.

von Lindern, M., Poustka, A., Lerach, H., and Grosveld, G. (1990). The (6;9) chromosome translocation, associated with a specific subtype of acute nonlymphocytic leukemia, leads to aberrant transcription of a target gene on 9q34. Mol. Cell. Biol. **10:** 4016–4026.

Waldmann, T., Eckerich, C., Baack, M., and Gruss, C. (2002). The ubiquitous chromatin protein DEK alters the structure of DNA by introducing positive supercoils. J. Biol. Chem. **277:** 24988–24994.

Waldmann, T., Baack, M., Richter, N., and Gruss, C. (2003). Structure-specific binding of the proto-oncogene protein DEK to DNA. Nucleic Acids Res. **31:** 7003–7010.

Waldmann, T., Scholten, I., Kappes, F., Hu, H.G., and Knippers, R. (2004). The DEK protein—an abundant and ubiquitous constituent of mammalian chromatin. Gene **343:** 1–9.

Wang, J.C. (2002). Cellular roles of DNA topoisomerases: a molecular perspective. Nat. Rev. Mol. Cell Biol. **3:** 430–440.

Wendt, K.S., and Peters, J.M. (2009). How cohesin and CTCF cooperate in regulating gene expression. Chromosome Res. **17:** 201–214.

Wise-Draper, T.M., Mintz-Cole, R.A., Morris, T.A., Simpson, D.S., Wikenheiser-Brokamp, K.A., Currier, M.A., Cripe, T.P., Grosveld, G.C., and Wells, S.I. (2009). Overexpression of the cellular DEK protein promotes epithelial transformation in vitro and in vivo. Cancer Res. **69:** 1792–1799.

Wollmann, H., Holec, S., Alden, K., Clarke, N.D., Jacques, P.-É., and Berger, F. (2012). Dynamic deposition of histone variant H3.3 accompanies developmental remodeling of the Arabidopsis transcriptome. PLoS Genet. **8:** e1002658.

Zhu, Y., Dong, A., and Shen, W.H. (2012). Histone variants and chromatin assembly in plant abiotic stress responses. Biochim. Biophys. Acta **1819:** 343–348.